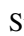




Early evolution constrained by high- p_{\perp} quark-gluon plasma tomographyStefan Stojku ¹, Jussi Auvinen ¹, Marko Djordjevic,² Pasi Huovinen ^{1,*} and Magdalena Djordjevic ^{1,†}¹*Institute of Physics Belgrade, National Institute of the Republic of Serbia, University of Belgrade, Serbia*²*Faculty of Biology, University of Belgrade, Serbia*

(Received 19 August 2020; revised 24 July 2021; accepted 25 January 2022; published 16 February 2022)

We show that high- p_{\perp} R_{AA} and v_2 are sensitive to the early expansion dynamics, and that the high- p_{\perp} observables prefer delayed onset of energy loss and transverse expansion. To calculate high- p_{\perp} R_{AA} and v_2 , we employ our newly developed DREENA-A framework, which combines state-of-the-art dynamical energy loss model with (3+1)-dimensional hydrodynamical simulations. The model applies to both light and heavy flavor, and we predict a larger sensitivity of heavy flavor observables to the onset of transverse expansion. This presents the first time when bulk QGP behavior has been constrained by high- p_{\perp} observables and related theory, i.e., by so-called QGP tomography.

DOI: [10.1103/PhysRevC.105.L021901](https://doi.org/10.1103/PhysRevC.105.L021901)

Quark-gluon plasma (QGP) [1,2] is an extreme form of matter that consists of interacting quarks, antiquarks, and gluons. This state of matter is formed in ultrarelativistic heavy-ion collisions at the Relativistic Heavy-Ion Collider (RHIC) and the Large Hadron Collider (LHC). When analyzing the heavy-ion collision data, the particles formed in these collisions are traditionally separated into high- p_{\perp} (rare hard probes) and low- p_{\perp} particles (bulk, consisting of 99.9% of particles formed in these collisions).

The QGP properties are traditionally explored by low- p_{\perp} observables [3–6], while rare high- p_{\perp} probes are, almost exclusively, used to understand the interactions of high- p_{\perp} partons with the surrounding QGP medium. High- p_{\perp} physics had a decisive role in the QGP discovery [7], but it has been rarely used to understand bulk QGP properties. On the other hand, some important bulk QGP properties are difficult to constrain by low- p_{\perp} observables and corresponding theory/simulations [8–11]. We are therefore advocating QGP tomography, where bulk QGP parameters are jointly constrained by low- and high- p_{\perp} physics.

During the last few years, our understanding of the very early evolution of QGP has evolved a lot. In particular the discovery of the attractor solutions of the evolution of nonequilibrated systems [12–14], and models based on effective kinetic theory [15,16] have been significant milestones. However, the exact dynamics of early evolution and hydrodynamization of the medium, i.e., the approach to the state where the system can be described using fluid dynamics, are not settled yet. Furthermore, to our knowledge, there are no reliable methods to calculate jet energy loss in a medium out of equilibrium. Instead of microscopic calculation of the early-time dynamics, we take a complementary approach in this Letter. We calculate the high- p_{\perp} R_{AA} and v_2 in a few

straightforward scenarios, and show how the comparison to high- p_{\perp} data constrains the early evolution.

In the attractor solutions, the final evolution is fluid dynamical even if the initial state is quite far from equilibrium. This allows us to entertain the notion that even if the early state is not in local equilibrium, we could use fluid dynamics to describe its evolution from very early times [17], say from $\tau_0 = 0.2$ fm, where τ_0 is the initial time of fluid dynamical evolution. Correspondingly, we may argue that the temperature entering fluid dynamical evolution controls also jet energy loss, and we may start the jet energy loss at the same time, $\tau_q = 0.2$ fm. On the other hand, we had studied the preequilibrium energy loss in various scenarios [18], and seen that even if the data could not properly distinguish these scenarios, Bjorken-type temperature evolution at very early times tended to push R_{AA} too low. This may suggest that applying the equilibrium jet-medium interactions to the preequilibrium stage (even if close enough to fluid dynamical) overestimates the energy loss. Due to this, we here, for simplicity, assume an opposite limit, where we start the energy loss later than the fluid dynamical evolution: $\tau_q = 1.0$ fm and $\tau_0 = 0.2$ fm.¹

Frequently used toy model to study the effects of early nonequilibrium evolution is the free-streaming approach [19,20], where (fictional) particles are allowed to stream freely until the initial time of fluid dynamical evolution τ_0 . As our third scenario, we allow free streaming until $\tau_0 = 1.0$ fm. Consistently with the assumed absence of interactions in the bulk medium, we assume no jet-medium interactions during the out-of-equilibrium stage, so that $\tau_0 = \tau_q = 1.0$ fm. For comparison's sake, we also explore the old-fashioned scenario where nothing happens before the fluid dynamical initial time $\tau_0 = \tau_q = 1.0$ fm, i.e., we start the fluid-dynamical evolution at $\tau = 1.0$ fm with zero transverse flow velocity.

^{*}pasi@ipb.ac.rs[†]magda@ipb.ac.rs¹Similar scenario was suggested and studied in Ref. [66].

When calculating how the high- p_{\perp} observables depend on our different scenarios we have to ensure that the QGP medium evolution is compatible with the observed distributions of low- p_{\perp} particles. We describe the medium evolution using the (3+1)-dimensional viscous hydrodynamical model [21]. For simplicity, we choose a constant shear viscosity to entropy density ratio $\eta/s = 0.12$ for the cases without pre-hydro transverse flow, and $\eta/s = 0.16$ for the free-streaming initialization. In all the cases the initial energy density profile in transverse plane is given by the binary collision density n_{BC} from the optical Glauber model:

$$e(\tau_0, x, y, b) = C_e(\tau_0)(n_{\text{BC}} + c_1 n_{\text{BC}}^2 + c_2 n_{\text{BC}}^3). \quad (1)$$

The parameters C_e , c_1 , and c_2 are tuned separately for each scenario, to approximately describe the observed charged particle multiplicities and $v_2\{4\}$ in Pb+Pb collisions at $\sqrt{s_{\text{NN}}} = 5.02$ TeV. For the longitudinal profile, we keep the parametrization used for $\sqrt{s_{\text{NN}}} = 2.76$ Pb+Pb collisions [21]. The equation of state is *s95p-PCE-v1* [22]. We use freeze-out temperatures $T_{\text{chem}} = 150$ MeV and $T_{\text{dec}} = 100$ MeV for cases without pre-hydro flow, but with free streaming we use $T_{\text{chem}} = 175$ MeV [23] to mimic bulk viscosity around T_c required to fit the p_T distributions, and $T_{\text{dec}} = 140$ MeV.

In the free-streaming initialization massless particles stream freely from $\tau = 0.2$ fm to $\tau_0 = 1.0$ fm, where the energy-momentum tensor based on the distributions of these particles is evaluated. The energy momentum tensor is decomposed to densities, flow velocity, and dissipative currents, which are used as the initial state of the subsequent fluid-dynamical evolution. The switch from massless noninteracting particles to strongly interacting constituents of QGP causes large positive bulk pressure at τ_0 . In our calculations bulk viscosity coefficient is always zero, and the initial bulk pressure will approach zero according to Israel-Stewart equations.

The transverse momentum distributions of charged particles are shown in Fig. 1, and p_{\perp} -differential elliptic flow parameter $v_2\{4\}(p_{\perp})$ in the low momentum part ($p_{\perp} < 2$ GeV) of the bottom panels of Fig. 2. As seen, the overall agreement with the data is acceptable.

To be able to use the high- p_{\perp} sector to study the bulk behavior we need a framework that incorporates both state-of-the-art energy loss and bulk medium simulations. With this goal, we recently developed a fully optimized modular framework DREENA-A [25], which can incorporate any, arbitrary, temperature profile within the dynamical energy loss formalism (outlined below). Consequently, ‘‘DREENA’’ stands for Dynamical Radiative and Elastic ENergy loss Approach, while ‘‘A’’ stands for Adaptive. The framework does not have fitting parameters within the energy loss model, allowing to fully exploit different temperature profiles (as the only input in the DREENA-A framework), systematically compare the data and predictions obtained by the same formalism and parameter set, and consequently constrain the bulk QGP properties from jointly studying low- and high- p_{\perp} theory and data.

The initial quark spectrum is computed at next-to-leading order [26] for light and heavy partons. To generate charged hadrons, we use DSS [27] fragmentation functions. For D and B mesons, we use BCFY [28] and KLP [29] fragmentation

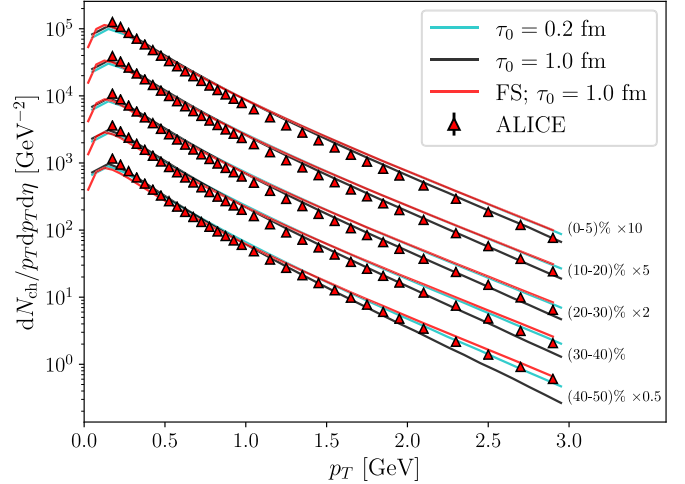


FIG. 1. Transverse momentum spectrum of charged particles in five centrality classes in Pb+Pb collisions at $\sqrt{s_{\text{NN}}} = 5.02$ TeV, with two initial times $\tau_0 = 0.2$ and $\tau_0 = 1.0$ fm, and free streaming initialization (FS). ALICE data from Ref. [24].

functions, respectively. In the presence of QCD medium, the vacuum fragmentation functions should be modified along with parton energy loss as described by the multiscale models [30,31]. However, for high- $p_{\perp} > 10$ GeV, which is the momentum region covered in our study,² such modification is small, justifying the use of vacuum fragmentation [30].

The dynamical energy loss formalism [32,33] has several unique features: (i) QCD medium of finite size and temperature consisting of dynamical (i.e., moving) partons; this in distinction to medium models with widely used static approximation and/or vacuumlike propagators [34–37]. (ii) Calculations based on generalized hard-thermal-loop approach [38], with naturally regulated infrared divergences [32,33,39]. (iii) Calculations of both radiative [32] and collisional [33] energy loss in the same theoretical framework. (iv) Generalization towards running coupling [40], finite magnetic mass [41]. We also recently advanced the formalism towards relaxing the widely used soft-gluon approximation [42]. All of these features are necessary for accurate predictions [43], but utilizing evolving temperature profiles is highly nontrivial within this complex energy loss framework.

We use the same parameter set to generate high- p_{\perp} predictions as in our earlier studies within DREENA-C [44] and DREENA-B [45] frameworks. In particular, we use $\Lambda_{\text{QCD}} = 0.2$ GeV and effective light quark flavors $n_f = 3$. For light quark mass, we assume to be dominated by the thermal mass $M = \mu_E/\sqrt{6}$, and for the gluon mass, we take $m_g = \mu_E/\sqrt{2}$ [39]. The temperature-dependent Debye mass μ_E is obtained by applying procedure from Ref. [46], which leads to results compatible with the lattice QCD [47]. The charm (bottom) mass is $M = 1.2$ GeV ($M = 4.75$ GeV). Magnetic to electric mass ratio is $0.4 < \mu_M/\mu_E < 0.6$ [48–51], but for simplicity

²As the assumptions in the dynamical energy loss break down below 10 GeV, we consider our predictions to be reliable in the region $p_{\perp} > 10$ GeV.

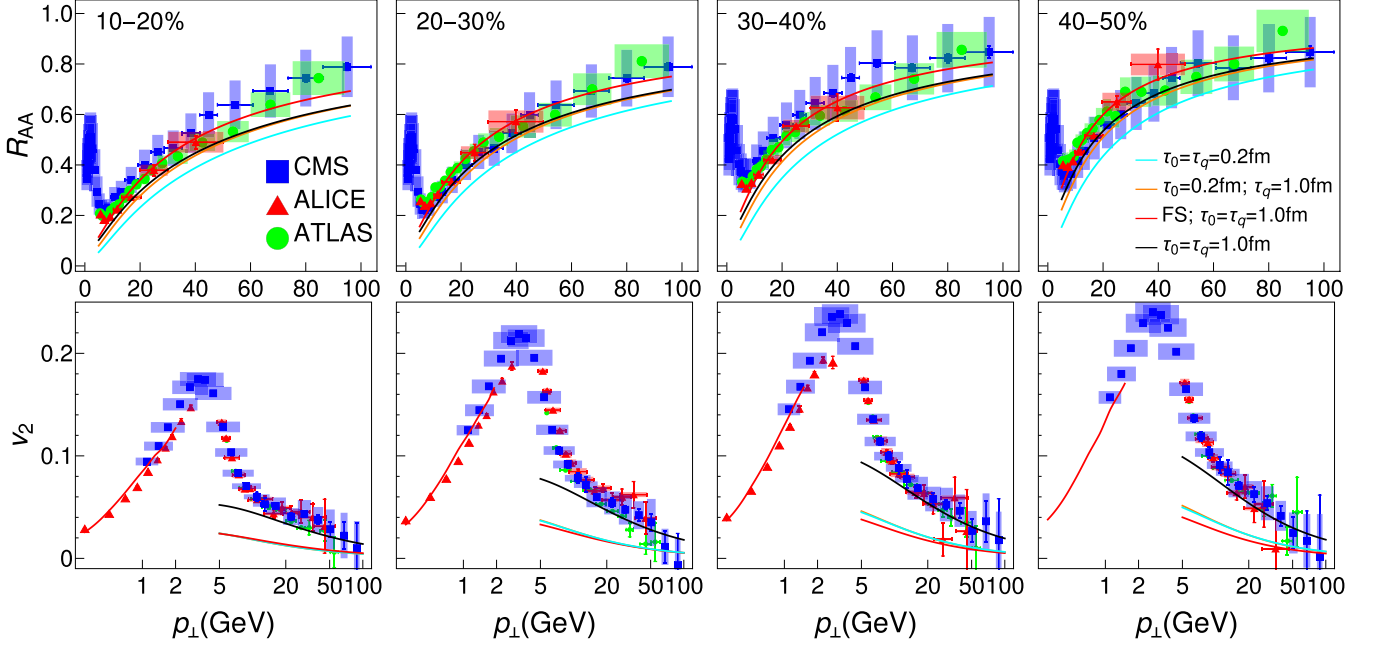


FIG. 2. Charged hadron DREENA-A R_{AA} (top panels) and v_2 (bottom panels) predictions, generated for different τ_0 , τ_q , and initialization (see the legend, FS stands for free streaming), are compared with ALICE [24,52], CMS [53,54], and ATLAS [55,56] data. Four columns, from left to right, correspond to 10–20 %, 20–30 %, 30–40 %, and 40–50 % centralities at $\sqrt{s_{NN}} = 5.02$ TeV Pb+Pb collisions at the LHC. At low p_{\perp} ($p_{\perp} < 2$ GeV) v_2 is 4-cumulant $v_2\{4\}$, whereas at high p_{\perp} ($p_{\perp} > 5$ GeV) we evaluate v_2 as $v_2 = (1/2)(R_{AA}^{\text{in}} - R_{AA}^{\text{out}})/(R_{AA}^{\text{in}} + R_{AA}^{\text{out}})$.

$\mu_M/\mu_E = 0.5$, leading to the uncertainty of up to 10% for both R_{AA} and v_2 results.

The resulting DREENA-A predictions for charged hadron R_{AA} and v_2 in four different centrality classes, and four scenarios of early evolution, are shown in Fig. 2, and compared with experimental data. As one can expect, the later the energy loss begins, the higher the R_{AA} , and evaluating the energy loss as in thermalized medium already at $\tau_q = 0.2$ fm is slightly disfavored. Furthermore, early free-streaming evolution leads to larger R_{AA} than fluid-dynamical evolution. On the other hand, the behavior of v_2 is different. First, if the early expansion is fluid dynamical, we see that delaying the onset of energy loss hardly changes v_2 at all. Second, early free-streaming evolution does not lead to better reproduction of the data, but, in peripheral collisions, the fit is even worse. The only case when our v_2 predictions approach the data, is when both the jet energy loss and the transverse expansion are delayed to $\tau = 1$ fm.

As shown in Fig. 3, heavy quarks are even more sensitive to the early evolution. For bottom probes, the data are largely not available, making these true predictions. For charm probes, the available experimental data are much more sparse (and with larger error bars) than the charged hadron data. However, where available, comparison of our predictions with the data suggests the same preference towards delayed energy loss and transverse expansion as charged hadrons. These results are important, as consistency between light and heavy flavor is crucial (though highly nontrivial, as, e.g., implied by the well-known heavy flavor puzzle [62]) for studying the QGP properties.

To investigate the origin of the sensitivity of R_{AA} and v_2 to the early evolution, we evaluate the temperature along

the paths of jets traveling in-plane ($\phi = 0$) and out-of-plane ($\phi = \pi/2$) directions, and average over all sampled jet paths. In Fig. 4 we show the time evolution of the average of temperatures in in- and out-of-plane directions, and their difference

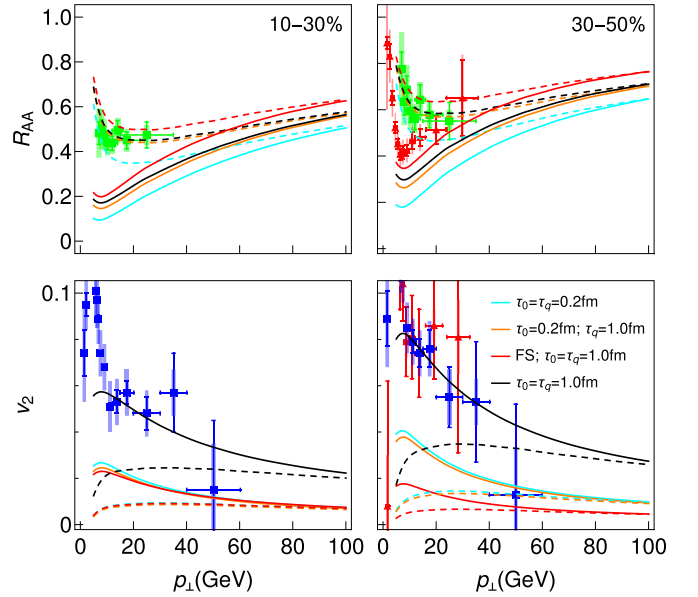


FIG. 3. Predicted D (full curves) and B meson (dashed curves) R_{AA} (top panels) and v_2 (bottom panels) in Pb+Pb collisions at $\sqrt{s_{NN}} = 5.02$ TeV. The predictions for D mesons are compared with ALICE [57,58] (red triangles) and CMS [59] (blue squares) D meson data, while predictions for B mesons are compared with CMS [60] (green circles) nonprompt J/Ψ data.

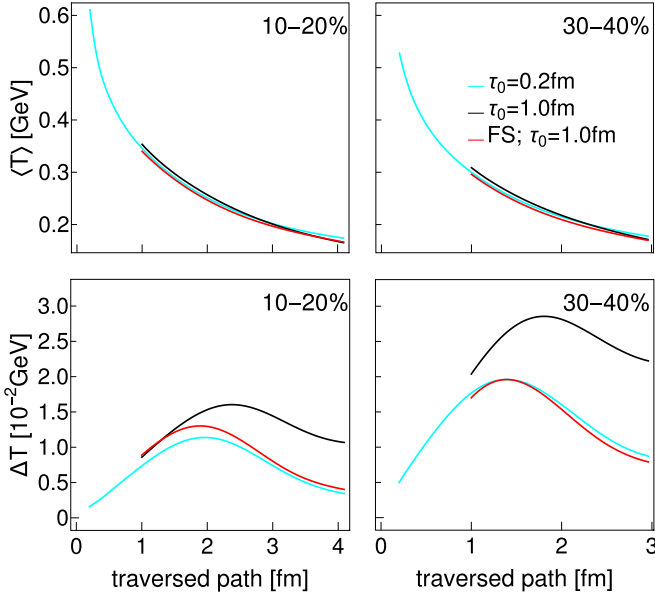


FIG. 4. Average temperature along the jet path traversing the system (top panel) and the difference of average temperatures in out-of-plane and in-plane directions (bottom panel) for $\tau_0 = 0.2$ and 1.0 fm and free-streaming initialization at 10–20 % and 30–40 % centrality classes. The average is over all sampled jet paths, and the path ends at $T_C \approx 160$ MeV [61].

in 10–20 % and 30–40 % central collisions for $\tau_0 = 0.2$ and 1.0 fm, and the free-streaming initialization. The behavior of R_{AA} is now easy to understand in terms of average temperature: Larger τ_q , i.e., delay in the onset of energy loss, cuts away the large temperature part of the profile decreasing the average temperature, and thus increasing the R_{AA} [44,45]. Similarly, for late start of transverse expansion, i.e., $\tau_0 = 1.0$ fm, the temperature is first slightly larger and later lower than for $\tau_0 = 0.2$ fm, and thus the R_{AA} in $\tau_0 = \tau_q = 1.0$ fm and $\tau_0 = 0.2$ with $\tau_q = 1.0$ cases is almost identical. On the other hand, due to the rapid expansion of the edges of the system, free-streaming initialization leads to lower average temperature than any other scenario, and thus to the largest R_{AA} .

High- p_\perp v_2 , on the other hand, is proportional to the difference in temperature along in-plane and out-of-plane directions, and to lesser extent to the average temperature. Delaying the onset of transverse expansion to $\tau_0 = 1.0$ fm leads to larger difference than either early fluid-dynamical or free-streaming expansion, and thus v_2 is largest in that case. As well, delaying the onset of energy loss by increasing τ_q hardly changes v_2 , since at early times the temperature seen by jets in in- and out-of-plane directions is almost identical, and no v_2 is built up at that time. Early free streaming and early fluid-dynamical expansion lead to similar differences in temperatures. The slightly larger difference in the 10–20 % centrality class is counteracted by slightly lower temperature, and thus final v_2 is practically identical in both cases. In the more peripheral 30–40 % class the differences in temperature are almost identical, but the lower average temperature leads to lower v_2 for free streaming.

The delay in transverse expansion affects the average temperature along the jet in two ways. First, smaller τ_0 means larger initial gradients, faster buildup of flow, and faster dilution of the initial spatial anisotropy. Similarly, free-streaming leads to even faster buildup of flow and dilution of spatial anisotropies than early fluid-dynamical expansion. Second, since the initial jet production is azimuthally symmetric, and jets travel along eikonal trajectories, at early times both in- and out-of-plane jets probe the temperature of the medium almost the same way. Only with course of time will the spatial distribution of in- and out-of-plane jets differ, and the average temperature along their paths begins to reflect the anisotropies of the fluid temperature. This qualitative understanding indicates that the obtained conclusions are largely model independent.

The idea of using high- p_\perp theory and data to explore QGP is not new, see, e.g., Refs. [63–73]. While some of these approaches can achieve a reasonable agreement with the data (see, e.g., [73–75]), this agreement relies on adjusting fitting parameter(s) in the energy loss model, which prevents them from constraining the bulk medium properties. These models thus largely concentrate on investigating the nature of parton interactions (e.g., a new phenomenon of magnetic monopoles is systematically introduced in Ref. [73]) rather than exploring which dynamical evolution better explains the data. In contrast, the goal of our approach is to constrain the bulk QGP behavior. The major advantage of our framework is that it does not use fitting parameters in the energy loss model, enabling us to explore the effects of different bulk medium evolutions. We can even use R_{AA} to make conclusions about the bulk properties of the system, where our R_{AA} results imply that the energy loss during the very early evolution is weaker than energy loss in a fully thermal system.

Furthermore, our study shows that not only is early energy loss suppressed [64,66], but the early buildup of transverse expansion must be delayed as well. It is not sufficient to delay cooling as suggested in Ref. [64], but the initial anisotropy must be diluted at much slower rate than given by either free streaming or by fluid dynamics. We do not expect current more sophisticated approaches to preequilibrium dynamics, such as $K\phi MP\phi ST$ based on effective kinetic theory [15,16], to resolve this issue. As seen in Ref. [76], except in most peripheral collisions, both $K\phi MP\phi ST$ and free streaming lead to very similar final distributions. Thus we may expect that at the time of switching to fluid dynamics, they both have lead to very similar flow and temperature profiles (and thus anisotropies).

Alternatively, the initial spatial anisotropies could be much larger than considered here. It is known that both IP-Glasma and EKRT approaches lead to larger eccentricities than Glauber, but we have tested that they both lead to too low high- p_\perp v_2 , if the fluid dynamical evolution begins as usually assumed in calculations utilizing IP-Glasma or EKRT initializations. Event-by-event fluctuations may enhance spatial anisotropies as well, and by generating shorter scale structures, they may enhance the sensitivity of high- p_\perp v_2 to spatial anisotropies. However, for these additional structures to enhance the high- p_\perp v_2 , they should be correlated with the event plane, which is not necessarily the case. While we have

postponed a study of event-by-event fluctuations to a further work, our preliminary results do not indicate substantial influence on high- p_{\perp} predictions.

In summary, we presented (to our knowledge) the first example of using high- p_{\perp} theory and data to provide constraints to bulk QGP evolution. Specifically, we inferred that experimental data suggest that at early times both the energy loss and transverse expansion of the system should be significantly weaker than in conventional models. We emphasize that the assumption that no energy loss nor transverse expansion takes place before $\tau_0 = 1.0$ fm is unrealistic. We are not advocating such a scenario, but note that the only way available to us to test our hypothesis that the early energy loss and expansion should be suppressed was to take the limit of no energy loss nor transverse expansion at all. Doing this significantly improves the agreement with the data, thus supporting our hypothesis. While our finding of delayed onset of energy loss

and transverse expansion has yet to be physically understood, there have been several anomalies in the history of heavy-ion physics, and our result is one more of them.

Furthermore, heavy flavor observables show large sensitivity to the details of early evolution, so our conclusion will be further tested by the upcoming high luminosity measurements. Our results demonstrate inherent interconnections between low- and high- p_{\perp} physics, strongly supporting the utility of our QGP tomography approach, where bulk QGP properties are jointly constrained by low- and high- p_{\perp} data.

This work is supported by the European Research Council, Grant No. ERC-2016-COG: 725741, and by the Ministry of Education, Science and Technological Development of the Republic of Serbia, under Projects No. ON171004 and No. ON173052.

-
- [1] J. C. Collins and M. J. Perry, *Phys. Rev. Lett.* **34**, 1353 (1975).
 [2] G. Baym and S. A. Chin, *Phys. Lett. B* **62**, 241 (1976).
 [3] D. A. Teaney, *Quark-Gluon Plasma* **4**, 207 (2010).
 [4] C. Shen, *Nucl. Phys. A* **1005**, 121788 (2021).
 [5] B. Jacak and P. Steinberg, *Phys. Today* **63**, 39 (2010).
 [6] C. V. Johnson and P. Steinberg, *Phys. Today* **63**, 29 (2010).
 [7] M. Gyulassy and L. McLerran, *Nucl. Phys. A* **750**, 30 (2005).
 [8] J. L. Nagle, I. G. Bearden, and W. A. Zajc, *New J. Phys.* **13**, 075004 (2011).
 [9] J. D. Orjuela Koop, A. Adare, D. McGlinchey, and J. L. Nagle, *Phys. Rev. C* **92**, 054903 (2015).
 [10] J. Auvinen, J. E. Bernhard, S. A. Bass, and I. Karpenko, *Phys. Rev. C* **97**, 044905 (2018).
 [11] J. Auvinen, K. J. Eskola, P. Huovinen, H. Niemi, R. Paatelainen, and P. Petreczky, *Phys. Rev. C* **102**, 044911 (2020).
 [12] M. P. Heller and M. Spalinski, *Phys. Rev. Lett.* **115**, 072501 (2015).
 [13] Y. Akamatsu, *Nucl. Phys. A* **1005**, 122000 (2021).
 [14] C. Shen and L. Yan, *Nucl. Sci. Tech.* **31**, 122 (2020).
 [15] A. Kurkela, A. Mazeliauskas, J. F. Paquet, S. Schlichting, and D. Teaney, *Phys. Rev. Lett.* **122**, 122302 (2019).
 [16] A. Kurkela, A. Mazeliauskas, J. F. Paquet, S. Schlichting, and D. Teaney, *Phys. Rev. C* **99**, 034910 (2019).
 [17] C. Chattopadhyay and U. W. Heinz, *Phys. Lett. B* **801**, 135158 (2020).
 [18] D. Zigic, B. Ilic, M. Djordjevic, and M. Djordjevic, *Phys. Rev. C* **101**, 064909 (2020).
 [19] W. Broniowski, W. Florkowski, M. Chojnacki, and A. Kisiel, *Phys. Rev. C* **80**, 034902 (2009).
 [20] J. Liu, C. Shen, and U. Heinz, *Phys. Rev. C* **91**, 064906 (2015); **92**, 049904(E) (2015).
 [21] E. Molnar, H. Holopainen, P. Huovinen, and H. Niemi, *Phys. Rev. C* **90**, 044904 (2014).
 [22] P. Huovinen and P. Petreczky, *Nucl. Phys. A* **837**, 26 (2010).
 [23] H. Niemi, K. J. Eskola, and R. Paatelainen, *Phys. Rev. C* **93**, 024907 (2016).
 [24] The ALICE collaboration, S. Acharya *et al.*, *J. High Energy Phys.* **11** (2018) 013.
 [25] D. Zigic, I. Salom, J. Auvinen, P. Huovinen, and M. Djordjevic, [arXiv:2110.01544](https://arxiv.org/abs/2110.01544) [nucl-th].
 [26] Z. B. Kang, I. Vitev, and H. Xing, *Phys. Lett. B* **718**, 482 (2012); R. Sharma, I. Vitev, and B. W. Zhang, *Phys. Rev. C* **80**, 054902 (2009).
 [27] D. de Florian, R. Sassot, and M. Stratmann, *Phys. Rev. D* **75**, 114010 (2007).
 [28] M. Cacciari and P. Nason, *J. High Energy Phys.* **09** (2003) 006; E. Braaten, K.-M. Cheung, S. Fleming, and T. C. Yuan, *Phys. Rev. D* **51**, 4819 (1995).
 [29] V. G. Kartvelishvili, A. K. Likhoded, and V. A. Petrov, *Phys. Lett. B* **78**, 615 (1978).
 [30] S. Cao, Y. Chen, J. Coleman, J. Mulligan, P.M. Jacobs, R.A. Soltz, A. Angerami, R. Arora, S.A. Bass, L. Cunqueiro, T. Dai, L. Du, R. Ehlers, H. Elfner, D. Everett, W. Fan, R. J. Fries, C. Gale, F. Garza, Y. He, M. Heffernan, U. Heinz, B.V. Jacak, S. Jeon, W. Ke, B. Kim, M. Kordell, A. Kumar, A. Majumder, S. Mak, M. McNelis, C. Nattrass, D. Oliinychenko, C. Park, J.F. Paquet, J.H. Putschke, G. Roland, A. Silva, B. Schenke, L. Schwiebert, C. Shen, C. Sirimanna, Y. Tachibana, G. Vujanovic, X.N. Wang, R.L. Wolpert, and Y. Xu, [JETSCAPE], *Phys. Rev. C* **104**, 024905 (2021).
 [31] W. Ke and X. N. Wang, *J. High Energy Phys.* **05** (2021) 041.
 [32] M. Djordjevic, *Phys. Rev. C* **80**, 064909 (2009); M. Djordjevic and U. Heinz, *Phys. Rev. Lett.* **101**, 022302 (2008).
 [33] M. Djordjevic, *Phys. Rev. C* **74**, 064907 (2006).
 [34] R. Baier, Y. Dokshitzer, A. Mueller, S. Peigne, and D. Schiff, *Nucl. Phys. B* **484**, 265 (1997).
 [35] N. Armesto, C. A. Salgado, and U. A. Wiedemann, *Phys. Rev. D* **69**, 114003 (2004).
 [36] M. Gyulassy, P. Lévai, and I. Vitev, *Nucl. Phys. B* **594**, 371 (2001).
 [37] X. N. Wang and X. F. Guo, *Nucl. Phys. A* **696**, 788 (2001).
 [38] J. I. Kapusta, *Finite-Temperature Field Theory* (Cambridge University Press, Cambridge, 1989).
 [39] M. Djordjevic and M. Gyulassy, *Phys. Rev. C* **68**, 034914 (2003).
 [40] M. Djordjevic and M. Djordjevic, *Phys. Lett. B* **734**, 286 (2014).
 [41] M. Djordjevic and M. Djordjevic, *Phys. Lett. B* **709**, 229 (2012).
 [42] B. Blagojevic, M. Djordjevic, and M. Djordjevic, *Phys. Rev. C* **99**, 024901 (2019).

- [43] B. Blagojevic and M. Djordjevic, *J. Phys. G* **42**, 075105 (2015).
- [44] D. Zigic, I. Salom, J. Auvinen, M. Djordjevic, and M. Djordjevic, *J. Phys. G* **46**, 085101 (2019).
- [45] D. Zigic, I. Salom, J. Auvinen, M. Djordjevic, and M. Djordjevic, *Phys. Lett. B* **791**, 236 (2019).
- [46] A. Peshier, [arXiv:hep-ph/0601119](https://arxiv.org/abs/hep-ph/0601119).
- [47] O. Kaczmarek, F. Karsch, F. Zantow, and P. Petreczky, *Phys. Rev. D* **70**, 074505 (2004); O. Kaczmarek and F. Zantow, *ibid.* **71**, 114510 (2005).
- [48] Y. Maezawa, S. Aoki, S. Ejiri, T. Hatsuda, N. Ishii, K. Kanaya, N. Ukita, and T. Umeda (WHOT-QCD Collaboration), *Phys. Rev. D* **81**, 091501(R) (2010).
- [49] A. Nakamura, T. Saito, and S. Sakai, *Phys. Rev. D* **69**, 014506 (2004).
- [50] A. Hart, M. Laine, and O. Philipsen, *Nucl. Phys. B* **586**, 443 (2000).
- [51] D. Bak, A. Karch, and L. G. Yaffe, *J. High Energy Phys.* **08** (2007) 049.
- [52] The ALICE collaboration, S. Acharya *et al.*, *J. High Energy Phys.* **07** (2018) 103.
- [53] V. Khachatryan, *et al.* [CMS], *J. High Energy Phys.* **04** (2017) 039.
- [54] A. M. Sirunyan, *et al.* [CMS], *Phys. Lett. B* **776**, 195 (2018).
- [55] [ATLAS], ATLAS-CONF-2017-012.
- [56] M. Aaboud *et al.* [ATLAS], *Eur. Phys. J. C* **78**, 997 (2018).
- [57] The ALICE collaboration, S. Acharya, *et al.*, *J. High Energy Phys.* **10** (2018) 174.
- [58] S. Acharya, *et al.* [ALICE], *Phys. Rev. Lett.* **120**, 102301 (2018).
- [59] A. M. Sirunyan, *et al.* [CMS], *Phys. Rev. Lett.* **120**, 202301 (2018).
- [60] A. M. Sirunyan, *et al.* [CMS], *Eur. Phys. J. C* **78**, 509 (2018).
- [61] A. Bazavov, T. Bhattacharya, C. DeTar, H.T. Ding, S. Gottlieb, R. Gupta, P. Hegde, U.M. Heller, F. Karsch, E. Laermann, L. Levkova, S. Mukherjee, P. Petreczky, C. Schmidt, C. Schroeder, R.A. Soltz, W. Soeldner, R. Sugar, M. Wagner, and P. Vranas (HotQCD Collaboration), *Phys. Rev. D* **90**, 094503 (2014).
- [62] M. Djordjevic, *J. Phys. G* **32**, S333-S342 (2006); M. Djordjevic and M. Djordjevic, *Phys. Rev. C* **90**, 034910 (2014).
- [63] I. Vitev and M. Gyulassy, *Phys. Rev. Lett.* **89**, 252301 (2002).
- [64] T. Renk, H. Holopainen, U. Heinz, and C. Shen, *Phys. Rev. C* **83**, 014910 (2011).
- [65] B. Betz and M. Gyulassy, *J. High Energy Phys.* **08** (2014) 090; **10** (2014) 043.
- [66] C. Andres, N. Armesto, H. Niemi, R. Paatelainen, and C. A. Salgado, *Phys. Lett. B* **803**, 135318 (2020).
- [67] S. Shi, J. Liao, and M. Gyulassy, *Chin. Phys. C* **42**, 104104 (2018).
- [68] K.M. Burke, A. Buzzatti, N. Chang, C. Gale, M. Gyulassy, U. Heinz, S. Jeon, A. Majumder, B. Muller, G.Y. Qin, B. Schenke, C. Shen, X.N. Wang, J. Xu, C. Young, and H. Zhang, [JET], *Phys. Rev. C* **90**, 014909 (2014).
- [69] A. Kumar, A. Majumder, and C. Shen, *Phys. Rev. C* **101**, 034908 (2020).
- [70] Y. He, T. Luo, X.-N. Wang, and Y. Zhu, *Phys. Rev. C* **91**, 054908 (2015); **97**, 019902(E) (2018).
- [71] S. Cao, T. Luo, G.-Y. Qin, and X.-N. Wang, *Phys. Rev. C* **94**, 014909 (2016).
- [72] J. Xu, A. Buzzatti, and M. Gyulassy, *J. High Energy Phys.* **08** (2014) 063.
- [73] S. Shi, J. Liao, and M. Gyulassy, *Chin. Phys. C* **43**, 044101 (2019).
- [74] W. Zhao, W. Ke, W. Chen, T. Luo, and X.-N. Wang, *Phys. Rev. Lett.* **128**, 022302 (2022).
- [75] K. Werner, I. Karpenko, M. Bleicher, T. Pierog, and S. Porteboeuf-Houssais, *Phys. Rev. C* **85**, 064907 (2012).
- [76] T. Nunes da Silva, D. Chinellato, M. Hippert, W. Serenone, J. Takahashi, G. S. Denicol, M. Luzum, and J. Noronha, *Phys. Rev. C* **103**, 054906 (2021).